STRUCTURAL CHEMISTRY

ISSN 2053-2296

Conformational disorder in the crystal structure of methyl 2-acetamido-2-deoxy-β-D-glucopyranosyl-(1→4)–2-acetamido-2-deoxy-β-D-glucopyranoside (methyl β-chitobioside) methanol monosolvate

Pradip Shit, Timothy Tetrault, Wenhui Zhang, Mi-Kyung Yoon, Allen G. Oliver and Anthony S. Serianni*

Department of Chemistry & Biochemistry, University of Notre Dame, Notre Dame, IN 46556-5670, USA. *Correspondence e-mail: aseriann@nd.edu

Received 2 May 2024
Accepted 31 May 2024

Edited by R. Diniz, Universidade Federal de Minas Gerais, Brazil

Keywords: crystal structure; methyl β-chitobioside; hydrogen bonding; conformational analysis.

CCDC reference: 2359730

Supporting information: this article has supporting information at journals.iucr.org/c

Methyl 2-acetamido-2-deoxy-β-D-glucopyranosyl-(1→4)-2-acetamido-2-deoxy-β-D-glucopyranoside (methyl β-chitobioside), (IV), crystallizes from aqueous methanol at room temperature to give a structure ($C_{17}H_{30}N_2O_{22}\cdot CH_3OH$) containing conformational disorder in the exocyclic hydroxymethyl group of one of its βGlcNAc residues. As observed in other X-ray structures of disaccharides containing β-(1→4) *O*-glycosidic linkages, inter-residue hydrogen bonding between O3H of the βGlcNAc bearing the OCH_3 aglycone and O5 of the adjacent βGlcNAc is observed based on the 2.79 Å internuclear distance between the O atoms. The structure of (IV) was compared to that determined previously for 2-acetamido-2-deoxy-β-D-glucopyranosyl-(1→4)-2-acetamido-2-deoxy-β-D-glucopyranose (β-chitobiose), (III). The *O*-glycosidic linkage torsion angles, *phi* (ϕ) and *psi* (ψ), in (III) and (IV) differ by 6–8°. The *N*-acetyl side chain conformation in (III) and (IV) shows some context dependence, with the C1—C2—N—C_{car} torsion angle 10–15° smaller for the βGlcNAc residue involved in the internal *O*-glycosidic linkage. In (IV), conformational disorder is observed in the exocyclic hydroxymethyl (–CH_2OH) group in the βGlcNAc residue bearing the OCH_3 aglycone, and a fitting of the electron density indicates an approximate 50:50 distribution of the *gauche–gauche* (*gg*) and *gauche–trans* (*gt*) conformers in the lattice. Similar behavior is not observed in (III), presumably due to the different packing structure in the vicinity of the –CH_2OH substituent that affects its ability to hydrogen bond to proximal donors/acceptors. Unlike (IV), a re-examination of the previously reported electron density of (III) revealed conformational disorder in the *N*-acetyl side chain attached to the reducing-end βGlcNAc residue caused by rotation about the C2—N bond.

1. Introduction

The reducing disaccharide 2-acetamido-2-deoxy-β-D-glucopyranosyl-(1→4)-2-acetamido-2-deoxy-α/β-D-glucopyranose, (I) (Fig. 1), is a building block in the construction of biologically important oligo- and polysaccharides. Disaccharide (I) is the repeating unit of the homopolysaccharide chitin, which is the primary component of the cell walls of fungi and the exoskeletons of crustaceans and insects (Moussian, 2019). In eukaryotic cells, including those of humans, (I) is a component of the *N*-glycans of glycoproteins, occurring in the $Man_3GlcNAc_2$ core pentasaccharide that is modified *in vivo* to give high-mannose, complex, and hybrid *N*-glycans (Esmail & Manolson, 2021). The *O*-glycosidic linkage in (I) is cleaved by the hydrolytic enzyme *endo*-β-*N*-acetylglucosaminidase (ENGase) *in vivo* in humans (Seki *et al.*, 2019; Klontz *et al.*, 2019). ENGase is a therapeutic target in the treatment of NGly1 disease, the latter caused by a defective or absent

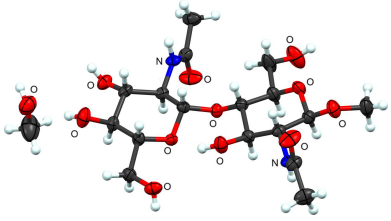

Table 1
Experimental details.

Crystal data	
Chemical formula	$C_{17}H_{30}N_2O_{11}·CH_4O$
M_r	470.47
Crystal system, space group	Monoclinic, $P2_1$
Temperature (K)	260
a, b, c (Å)	4.7599 (1), 14.3223 (5), 16.6515 (5)
β (°)	90.022 (2)
V (Å^3)	1135.18 (6)
Z	2
Radiation type	Cu $K\alpha$
μ (mm^{-1})	0.99
Crystal size (mm)	0.26 × 0.04 × 0.02
Data collection	
Diffractometer	Bruker Venture
Absorption correction	Numerical (*SADABS2016*; Krause *et al.*, 2015)
T_{min}, T_{max}	0.825, 1.0
No. of measured, independent and observed [$I > 2\sigma(I)$] reflections	20006, 4462, 4410
R_{int}	0.048
(sin $\theta/\lambda)_{max}$ (Å^{-1})	0.619
Refinement	
$R[F^2 > 2\sigma(F^2)]$, $wR(F^2)$, S	0.031, 0.080, 1.04
No. of reflections	4462
No. of parameters	330
No. of restraints	1
H-atom treatment	H atoms treated by a mixture of independent and constrained refinement
$\Delta\rho_{max}$, $\Delta\rho_{min}$ (e Å^{-3})	0.19, −0.14
Absolute structure	Twinning involves inversion, so Flack parameter cannot be determined

Computer programs: *APEX4* (Bruker, 2023), *SAINT* (Bruker, 2023), *SHELXT2018* (Sheldrick, 2015*a*), *SHELXL2019* (Sheldrick, 2015*b*), *Mercury* (Macrae *et al.*, 2020), and *FinalCIF* (Kratzert, 2023).

cytosolic peptide:*N*-glycanase (NGly1) (Pandey *et al.*, 2022). Disaccharide (I) is an inhibitor of the enzyme lysozyme (Fujihira *et al.*, 2017).

The X-ray crystal structures of the reducing disaccharides 2-acetamido-2-deoxy-β-D-glucopyranosyl-(1→4)-2-acetamido-2-deoxy-α-D-glucopyranose (α-chitobiose), (II), and 2-acetamido-2-deoxy-β-D-glucopyranosyl-(1→4)-2-acetamido-2-deoxy-β-D-glucopyranose, (III) (β-chitobiose), and of methyl 2-acetamido-2-deoxy-β-D-glucopyranoside, (V), have been reported (Fig. 1) (Mo & Jensen, 1978; Mo, 1979; Hu *et al.*, 2011). The interpretation of the diffraction data for (II) was complicated by disorder at the reducing end ($\alpha/\beta \sim 90/10$), and similar concerns may also pertain to (III). To eliminate this complication, the methyl glycoside of (III), *i.e.* methyl 2-acetamido-2-deoxy-β-D-glucopyranosyl-(1→4)-2-acetamido-2-deoxy-β-D-glucopyranoside, (IV) (methyl β-chitobioside) (Fig. 1), was prepared and found to give small crystals from aqueous methanol, from which a high-quality structure was obtained. In this article, the structural parameters in (II)–(V) are compared, with particular focus on linkage and side chain conformation, and structural disorder. A key finding is that, unlike that of the structurally-related (III), the crystal structure of (IV) contains conformational disorder at the C6 exocyclic hydroxymethyl (–CH_2OH) group of residue A (Fig. 1), with the *gauche–gauche* (*gg*) and *gauche–trans* (*gt*) rotamers nearly equally populated in the lattice.

2. Experimental

Crystal data, data collection and structure refinement details are summarized in Table 1. Data were recorded at 260 K on a Bruker Venture Kappa-geometry instrument equipped with a Cu-Diamond microfocus source and a Photon-III detector (Bruker, 2023). Lower temperatures were found to cause distortions in the crystal that resulted in a poorer data set and poorer model of the structure. The crystal was found to be twinned by merohedry perpendicular to the *a*-axis (twin law: $\bar{1}00$ 010 001; domain ratio = 0.51:0.49). This twin ratio does not allow for Bijvoet pair analysis and the correct configuration was determined by comparison with the known stereochemistry of the chemically synthesized (IV).

The structure was solved by dual-space methods (Sheldrick, 2015*a*) and routinely refined (Sheldrick, 2015*b*) (Table 1). Non-H atoms were modeled with anisotropic displacement parameters. H atoms bonded to C atoms were included in geometrically calculated positions, with $U_{iso}(H) = 1.2U_{eq}(C)$ and C—H bond distances restrained to 0.98–0.99 Å. Hydroxyl H atoms were included in observed positions and refined freely.

The notable feature of the molecular structure of (IV) was disorder in the position of atom O6. This disorder was modeled over two sites rotated ∼120° apart. The occupancy was initially refined summed to unity. However, that value refined very close to a 50:50 ratio and was set to this ratio in the final model. No other constraints were applied to the model.

3. Results and discussion

Selected structural parameters in the X-ray structure of (IV) (Fig. 2) are compared to the corresponding parameters in the X-ray structures of (II), (III), and (V) in Table 2. In this group of structures, the exocyclic C5—C6 bond lengths (1.509 ± 0.007 Å; averaged value ±1 standard deviation) are, on average, shorter than the endocyclic C—C bond lengths (1.526 ± 0.007 Å). The average C1—O1 (external and internal glycosidic), C1—O5, C4—O4, C4—O1′ (internal glycosidic), and C5—O5 bond lengths are 1.385 ± 0.011, 1.421 ± 0.005, 1.423 ± 0.003, 1.444 ± 0.006, and 1.434 ± 0.006 Å, respectively. Thus, the C1—O1 bond (internal and external glycosidic) is the shortest C—O bond in these structures, and the C5—O5 and C4—O1′ (internal glycosidic) bonds are the longest. The two C—O bonds that comprise the internal *O*-glycosidic linkages of (II)–(IV) include the shortest (relevant to linkage torsion angle ϕ) and longest (relevant to linkage torsion angle ψ) C—O bonds in these molecules [see Fig. 1 for the definitions of ϕ and ψ in (II)–(IV)].

In (II)–(V), the N1—C_{car} bond length averages 1.335 ± 0.011 Å and the C_{car}—O_{car} bond length averages 1.234 ± 0.009 Å. The C2—N1—C_{car}, N1—C_{car}—O_{car}, and O_{car}—C_{car}—C_{Me} bond angles in the *N*-acetyl side chains are similar (average value of 122.48 ± 1.26°), whereas the

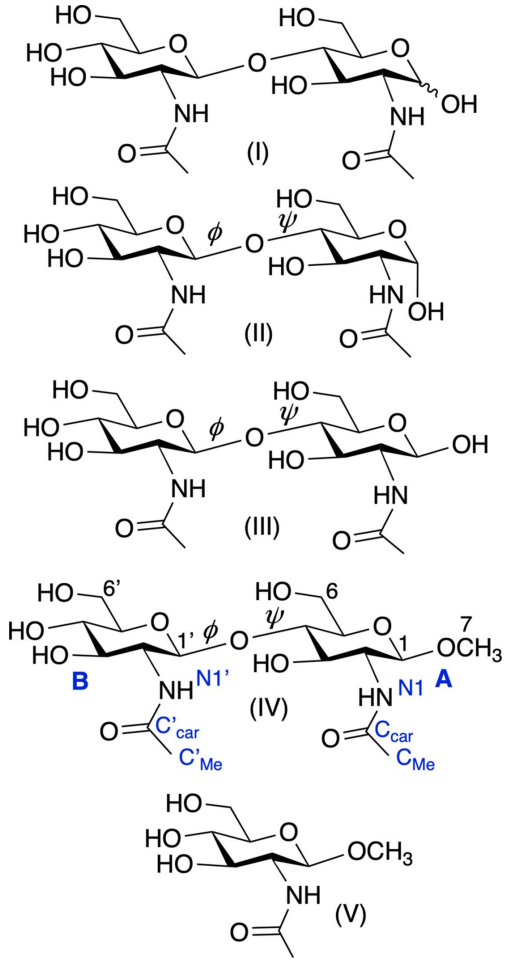

Figure 1
Structures of chitobiose, (I), α-chitobiose, (II), β-chitobiose, (III), methyl β-chitobioside, (IV), and methyl *N*-acetyl-β-D-glucosaminide, (V). Atom numbering and the assignments of residues A and B shown in (IV) apply to (I)–(III) and (V). The ϕ and ψ *O*-glycosidic linkage torsion angles are shown in (II)–(IV).

N1—C_{car}—C_{Me} bond angle averages to a significantly lower value of 115.97 ± 0.35°. The *N*-acetyl side chain adopts the *trans* configuration in (II)–(V) characterized by an average C2—N1—C_{car}—C_{Me} torsion angle of 176.7 ± 2.9° (absolute value).

Inter-residue hydrogen bonding is present in (II)–(IV), with O3H of residue A in each disaccharide serving as a donor to O5′ of residue B, although the O3—O5′ inter-residue distances are shorter in (III) and (IV) (2.789 and 2.796 Å, respectively) than in (II) (3.311 Å), implying stronger interactions in the former. Relatively short internuclear distances between O3 and O1′, and/or between O3 and O6′, are also observed in (II)–(IV) (2.8–3.3 Å), suggesting the presence of hydrogen bonding between these atoms. In (II), the O3—O1′ distance is much shorter than the O3—O5′ (and O3—O6′) distances, unlike the behavior observed in (III) and (IV). This latter difference is likely caused by different linkage torsion angles, ϕ and ψ, in (II)–(IV) as discussed below.

The endocyclic C5—O5—C1 bond angles in the βGlcNAcOCH$_3$, βGlcNAcO*R*, and βGlcNAcOH rings of (II)–(V) average 112.38 ± 0.43°, whereas the same angle is 114.49° in residue A of (II), which is an αGlcNAcOH ring. A similar pattern is observed for the exocyclic O5—C1—O1 bond angle, which averages 107.67 ± 0.56° in the βGlcNAcOCH$_3$, βGlcNAcO*R*, and βGlcNAcOH rings in (II)–(IV), and is much smaller than the value of 112.46° observed in the αGlcNAcOH ring of (II). In both cases, the anomeric configuration appears to be the main factor responsible for the differences and not whether the anomeric hydroxyl group is involved in the glycosidic linkage. The exocyclic C1—O1—CH$_3$ bond angle averages 112.92 ± 0.89° in (IV) and (V), whereas the structurally-related but inter-residue C1′—O1′—C4 bond angles average 116.48 ± 0.53° in (II)–(IV). The larger value of the latter is likely caused, at least in part, by the greater steric hindrance imposed on the internal *O*-glycosidic linkage.

The dispositions of the *N*-acetyl side chains with respect to the GlcNAc rings in (II)–(V) vary widely, as indicated by the C1—C2—N1—C_{car} torsion angles ranging from 100.0 to 115.7° for the βGlcNAc rings and 138.7° for the αGlcNAc ring in (II).

The internal *O*-glycosidic linkages in (II)–(IV) are characterized by two torsion angles, ϕ and ψ (Table 2). The values of ϕ_a (defined as C2′—C1′—O1′—C4; Table 2) range from 146.23 to 161.49°, while the values of ψ_a (defined as C1′—O1′—C4—C3; Table 2) range from 77.27 to 133.47°. The linkage conformations in (II)–(IV) are sufficiently different so as to produce different structural parameters associated with inter-residue hydrogen bonding between O3 and O5′ in (II)–(IV), as discussed above.

The conformation of the exocyclic hydroxymethyl group (–CH$_2$OH) in (II)–(V) varies considerably. In the two molecules of monosaccharide (V) observed in the crystal (V_A and V_B), the *gt* conformation (C4 *anti* to O6) is adopted, whereas in disaccharide (II), both GlcNAc residues adopt the *gg* conformation (H5 *anti* to O6). In (III), residue A adopts the *gg* conformation and residue B adopts the *gt* conformation. Although disaccharides (III) and (IV) differ only with respect to the structure of residue A [this residue bears a free ano-

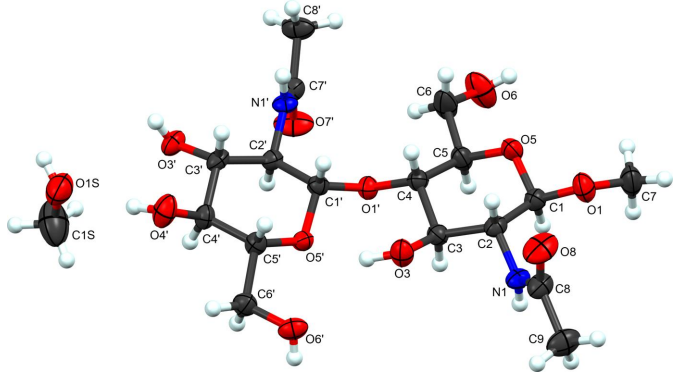

Figure 2
The molecular structure of (IV), showing the atom numbering. Atomic displacement ellipsoids are drawn at the 50% probability level and H atoms are shown as small spheres of arbitrary radii. The exocyclic hydroxymethyl group in residue A (see Fig. 1) is depicted in one of two conformations (*gt*) populated in the crystal.

Table 2
Selected structural parameters in the X-ray crystal structures of (II)–(V).

Structural parameter	Disaccharides						Monosaccharides	
	βGlcNAcOCH$_3$ (IV) (residue A)[b]	βGlcNAcO*R* (IV) (residue B)	βGlcNAcOH (III) (residue A)	βGlcNAcOR (III) (residue B)	βGlcNAcOH (II) (residue A)	αGlcNAcOR (II) (residue B)	βGlcNAcOCH$_3$ (V$_A$)[c]	βGlcNAcOCH$_3$ (V$_B$)[c]
Bond lengths (Å)								
C1—C2	1.531	1.533	1.522	1.522	1.526	1.515	1.533	1.531
C2—C3	1.534	1.535	1.521	1.531	1.527	1.517	1.530	1.534
C3—C4	1.536	1.527	1.531	1.516	1.520	1.516	1.527	1.525
C4—C5	1.529	1.530	1.536	1.507	1.519	1.537	1.526	1.523
C5—C6	1.503	1.508	1.501	1.499	1.512	1.516	1.519	1.514
C1—O1	1.376	1.394	1.389	1.389	1.361	1.395	1.389	1.387
C1—O5	1.416	1.420	1.427	1.429	1.418	1.414	1.418	1.423
C2—N1	1.443	1.444	1.450	1.446	1.450	1.460	1.456	1.455
C3—O3	1.420	1.419	1.430	1.424	1.421	1.431	1.430	1.424
C4—O4/O1′	1.437	1.418	1.448	1.425	1.448	1.422	1.424	1.425
C5—O5	1.428	1.436	1.429	1.436	1.438	1.427	1.443	1.435
C6—O6	*f*	1.436	1.413	1.415	1.419	1.423	1.430	1.430
O1—CH$_3$	1.435						1.445	1.439
N1—C$_{car}$	1.338	1.342	1.332	1.321	1.345	1.317	1.342	1.343
C$_{car}$—O$_{car}$	1.235	1.215	1.243	1.246	1.231	1.230	1.237	1.235
C$_{car}$—C$_{Me}$	1.499	1.501	1.497	1.495	1.490	1.506	1.508	1.510
O3···O5′	2.789		2.796		3.311			
O3···O1′	3.022		3.099		2.886			
O3···O6′	3.212		2.875		4.828			
Bond angles (°)								
C5—O5—C1	112.73	112.59	112.59	112.13	114.49	112.92	111.9	111.8
O5—C1—O1	108.71	107.32	107.71	106.87	112.46	107.68	107.64	107.76
C1—O1—CH$_3$	113.95						112.39	112.43
C1′—O1′—C4		116.03		117.07		116.34		
C2—N1—C$_{car}$	123.48	123.11	122.90	124.91	124.83	123.89	122.6	121.8
N1—C$_{car}$—C$_{Me}$	116.08	115.86	116.33	115.91	115.29	115.80	116.1	116.4
N1—C$_{car}$—O$_{car}$	121.85	122.69	121.49	121.26	123.94	123.89	122.6	122.9
O$_{car}$—C$_{car}$—C$_{Me}$	122.05	121.43	122.17	122.73	120.73	120.24	121.3	120.7
O3—H···O5′	154.85		132.75		142.95			
Torsion angles (°)								
C1—C2—C3—C4	−50.35	−50.20	−52.05	−48.16	−54.44	−56.66	−47.9	−50.1
C1—O5—C5—C4	65.26	61.07	61.82	67.41	60.36	59.12	69.3	66.5
C3—C4—C5—O5	−59.09	−47.51	−54.82	−58.61	−55.73	−54.68	−63.90	−56.56
O5—C5—C6—O6	*e*	60.73 (*gt*)	−60.61 (*gg*)	58.55 (*gt*)	−74.59 (*gg*)	−65.53 (*gg*)	64.3 (*gt*)	65.2 (*gt*)
C1—C2—N1—C$_{car}$	105.61	115.67	100.50	113.72	138.69	100.49	108.2	100.0
C3—C2—N1—C$_{car}$	−131.52	−123.42	−135.18	−122.48	−98.90	−136.95	−128.1	−137.2
C2—N1—C$_{car}$—C$_{Me}$	−177.54	172.27	−173.70	178.39	−179.61	−173.90	179.1	−179.1
H2—C2—N1—C$_{car}$	−12.83	−4.69	−12.50	−6.73	24.94	−16.95	−9.80	−19.20
C2—N1—C$_{car}$—O$_{car}$	4.14	−6.30	5.16	−5.28	−2.07	2.94	−1.2	0.8
C2—C3—O3—H	−179.52	−136.70	−148.65	−152.13	143.25	−51.20	−157.87	−112.65
C4—C3—O3—H	59.88	98.72	91.57		23.13			
H3—C3—O3—H	−61.48	−19.09	−31.91		−97.92			
C3—C4—O4—H		77.12		125.98		99.93	70.45	56.71
C5—C6—O6—H	*f*	−143.44	80.71	−178.65	88.34	−91.61	−80.28	−80.95
C2—C1—O1—CH$_3$/H (ϕ_a')[a]	159.18		161.75		−163.57		169.48	175.49
O5—C1—O1—CH$_3$/H (ϕ_b')	−81.33		−80.33		74.69		−71.05	−66.63
H1—C1—O1—CH$_3$/H (ϕ_c')	39.18		40.24		−42.50		49.18	54.04
C2′—C1′—O1′—C4 (ϕ_a)		146.23		151.65		161.49		
O5′—C1′—O1′—C4 (ϕ_b)		−95.82		−90.28		−79.57		
H1′—C1′—O1′—C4 (ϕ_c)		24.26		30.20		36.30		
C1′—O1′—C4—C3 (ψ_a)		84.73		77.27		133.47		
C1′—O1′—C4—C5 (ψ_b)		−154.81		−162.31		−106.89		
C1′—O1′—C4—H4 (ψ_c)		−36.73		−44.86		11.69		

Notes: (*a*) *O*-glycosidic torsion angles ϕ', ϕ, and ψ, which specify the rotational properties of the C1—O1, C1′—O1′, and O1′—C4 bonds, respectively, in (II)–(IV) can be defined by three different vicinal pathways, which are distinguished by the *a*–*c* subscripts. (*b*) See Fig. 1 for the definitions of residues A and B in (II)–(IV). For simplicity, C$_{car}$ and C$_{Me}$ are used in place of the *N*-acetyl side chain atom labeling in (IV) shown in Fig. 2. (*c*) (V$_A$) and (V$_B$) refer to the two molecules of (V) observed in the crystal structure (Hu *et al.*, 2011). (*d*) Data for (II), (III), and (V) were taken from Mo & Jensen (1978), Mo (1979), and Hu *et al.* (2011), respectively. (*e*) This torsion angle is disordered in the crystal, with approximately equal populations of *gg* and *gt*. (*f*) Could not be determined due to disorder of the O5—C5—C6—O6 torsion angle.

meric hydroxyl group in the β-configuration in (III), whereas it is a methyl glycoside in the β-configuration in (IV)], the behavior of the hydroxymethyl group differs in the two structures. Like residue B in (III), residue B in (IV) adopts the *gt* conformation, but unlike (III), conformational disorder is observed in the –CH$_2$OH group of residue A in (IV), with ∼50% of the molecules adopting the *gt* conformation and ∼50% adopting the *gg* conformation. In (III), atom O6 of

Table 3
Cremer–Pople puckering parameters for GlcNAc pyranosyl rings in (II)–(V).

Compound[a]	θ (°)	φ (°)	Q (Å)	q_2 (Å)	q_3 (Å)	Conformer[b]
(II), residue A	0.6 (3)	52.5 (3)	0.572 (3)	0.00,6 (3)	0.572 (3)	$B_{C1,C4}$
(II), residue B	2.9 (3)	96.5 (6)	0.580 (3)	0.029 (3)	0.580 (3)	$^{C5}S_{C1}$
(III), residue A	4.4 (3)	18.5 (4)	0.568 (3)	0.044 (3)	0.566 (3)	$^{C3}S_{C1}$
(III), residue B	8.8 (3)	338.1 (2)	0.577 (3)	0.088 (9)	0.570 (3)	$^{O5}S_{C2}$
(IV), residue A	5.2 (3)	324 (3)	0.581 (3)	0.055 (3)	0.579 (3)	$^{O5}S_{C2}$
(IV), residue B	12.1 (3)	45.8 (14)	0.564 (3)	0.121 (3)	0.552((3)	$B_{C1,C4}$
(V_A)	11.4 (3)	302.0 (12)	0.595 (3)	0.117 (3)	0.583 (3)	$B_{C2,C5}$
(V_B)	7.6 (2)	0.6 (2)	0.585 (3)	0.078 (2)	0.580 (3)	$^{C3,O5}B$

Notes: (*a*) see Fig. 1 for the definitions of residues A and B in disaccharides (II)–(IV). (*b*) *B* = boat and *S* = twist-boat or skew. Parameters shown for (II), (III), and (V) were extracted from crystal structures reported in Mo & Jensen (1978), Mo (1979), and Hu *et al.* (2011), respectively.

Table 4
Hydrogen-bond geometry (Å, °).

D—H···A	D—H	H···A	D···A	D—H···A
O6—H6O···O8^{i}	0.82	2.04	2.823 (7)	160
N1—H1N···O8^{ii}	0.84 (4)	2.02 (4)	2.829 (4)	160 (3)
C9—H9*A*···O5^{iii}	0.96	2.59	3.525 (5)	165
C9—H9*B*···O8^{ii}	0.96	2.57	3.398 (5)	144
O3′—H3′O···O6′^{iv}	0.83 (6)	1.88 (6)	2.692 (3)	165 (5)
O3—H3O···O5′	0.91 (5)	1.94 (5)	2.789 (3)	155 (4)
O3—H3O···O6′	0.91 (5)	2.55 (5)	3.212 (4)	130 (4)
O4′—H4′O···O1*S*	0.92 (5)	1.88 (5)	2.739 (4)	155 (5)
O6′—H6′O···O3′^{v}	0.76 (8)	1.99 (8)	2.750 (4)	173 (7)
N1′—H1N′···O7′^{vi}	0.93 (4)	1.88 (4)	2.808 (3)	171 (3)
C6′—H6′*A*···O7′^{v}	0.97	2.66	3.366 (5)	130
C8′—H8′*C*···O7′^{vi}	0.96	2.50	3.347 (5)	147
O1*S*—H1*S*···O3^{iv}	0.82	2.13	2.950 (4)	173
C1*S*—H1*SC*···O8^{iv}	0.96	2.56	3.371 (7)	142

Symmetry codes: (i) $-x+1, y+\frac{1}{2}, -z+2$; (ii) $x+1, y, z$; (iii) $-x+1, y-\frac{1}{2}, -z+2$; (iv) $-x+1, y+\frac{1}{2}, -z+1$; (v) $-x+2, y-\frac{1}{2}, -z+1$; (vi) $x-1, y, z$.

residue A serves as a hydrogen-bond mono-acceptor and donor to adjacent molecules of (III) in the lattice, and O6 of residue B serves as a mono-acceptor in an inter-residue hydrogen bond to O3H of residue A and a donor to a water molecule in the lattice. Thus, two hydrogen bonds to both O6 atoms in (III) anchor the hydroxymethyl groups in either the *gg* (residue A) or the *gt* (residue B) conformation. In (IV), atom O6 of residue B serves as a hydrogen-bond mono-acceptor and a donor to two adjacent molecules of (IV) in the lattice and, like residue B in (III), the –CH_2OH conformation is uniformly *gt* in this residue. However, in residue A of (IV), the –CH_2OH group adopts a *gt* conformation that is stabilized by a single hydrogen bond between atom O6 and the carbonyl O atom in the *N*-acetyl side chain of a proximal molecule of (IV). In the alternate *gg* conformation, no apparent hydrogen-bond donors or acceptors are evident from a visual inspection of the crystal packing, but ample space is available to allow the C5—C6 bond to adopt the *gg* conformation in the crystal. Apparently, the combination of only a single hydrogen bond stabilizing the *gt* form, and no hydrogen bonds stabilizing the *gg* form but ample space available to adopt the *gg* state, allows conformational disorder in the crystal of (IV) but not in (III).

The structure reported previously for (III) (Mo, 1979) was re-examined to confirm the lack of disorder at O6 of residue A. Examination of the model provided no evidence of this disorder, confirming that its behavior differs from that of (IV) in this respect. However, disorder in the *N*-acetyl side chain of residue A of (III) was detected, characterized by rotation of the C2—N1 bond, with the C1—C2—N1—C_{car} torsion angle adopting limiting values of 113.7 and 163.0°. This side chain disorder was not observed in (IV).

Cremer–Pople puckering parameters for the GlcNAc aldopyranosyl rings in (II)–(V) are shown in Table 3. Values of θ (a measure of the extent of ring distortion from an idealized $^4C_1$ chair form) vary from 0.9 to 12.1°. The aldohexopyranosyl ring of residue B in (II)–(IV) experiences greater distortion than the ring of residue A in each structure, and the ring distortion in (III) and (IV) is greater overall than that in (II), especially for residue B. The values of ϕ, which indicate the

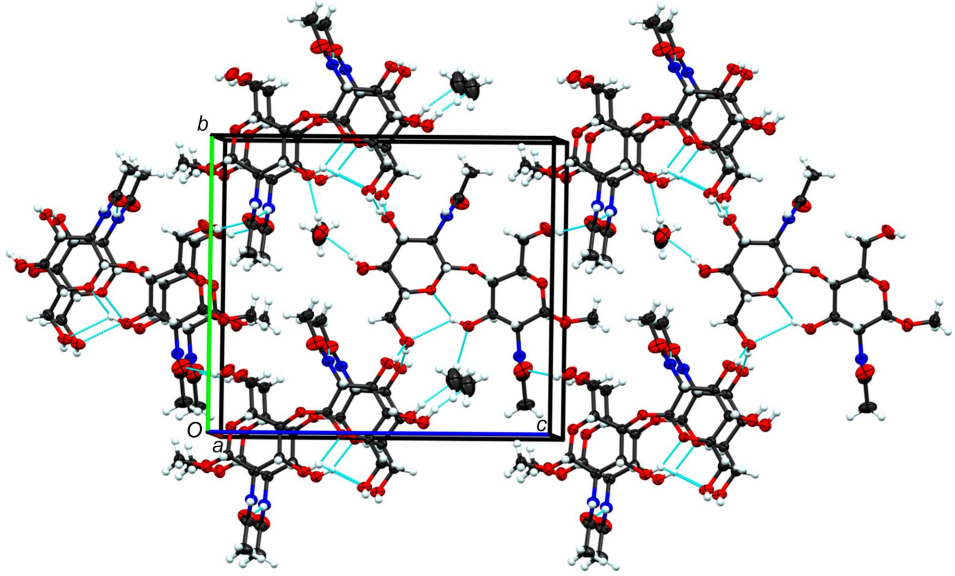

Figure 3
The packing diagram of (IV) viewed along the *a* axis. The blue dashed lines indicate hydrogen bonds.

direction of ring distortion, are clustered between 0–90 and 300–360°. The aldohexopyranosyl rings in (III) and (IV) differ in terms of the direction of distortion, with residue A giving ϕ values of 19 and 324°, and residue B giving values of 338 and 46° in (III) and (IV), respectively.

The three-dimensional (3D) hydrogen-bonded network for (IV) is formed by hydroxyl and amide hydrogen bonds (Fig. 3 and Table 4). Each amide N atom forms a hydrogen bond to the neighboring symmetry-related amide carbonyl O atom of that amide group [*i.e.* N1···O8^{ii} and N1′···O7′^{vi}; symmetry codes: (ii) $x + 1, y, z$; (vi): $x - 1, y, z$]. Hydroxyl O3 forms bifurcated hydrogen bonds to adjacent ring oxygen O5′ and hydroxyl O6′. Hydroxyl atom O3 also serves as an acceptor of a hydrogen bond from the methanol solvate (O1*S*···O3). Hydroxyl atom O4′ is the donor in the hydrogen bond to methanol solvent atom O1*S*. Hydroxyl atom O6 is a donor to the second hydrogen bond to a neighboring amide carbonyl O atom, O8. The alternate position of O6, *i.e.* O6*A*, is not oriented to form any hydrogen bonds. Atoms O3′ and O6′ serve as both donors and acceptors of hydrogen bonds of the same atoms, supporting the extension of the 3D nature along the *a* axis in conjunction with the amide hydrogen bonds described above.

Funding information

Funding for this research was provided by: National Science Foundation, Chemistry of Life Processes (award Nos. CHE-1707660 and CHE-2002625 to Anthony S. Serianni); National Science Foundation, Major Research Instrumentation (award No. CHE-2214606 to Allen G. Oliver).

References

Bruker (2023). *APEX4* and *SAINT*. Bruker AXS Inc., Madison, Wisconsin, USA.
Esmail, S. & Manolson, M. F. (2021). *Eur. J. Cell Biol.* **100**, 151186.
Fujihira, H., Masahara-Negishi, Y., Tamura, M., Huang, C., Harada, Y., Wakana, S., Takakura, D., Kawasaki, N., Taniguchi, N., Kondoh, G., Yamashita, T., Funakoshi, Y. & Suzuki, T. (2017). *PLoS Genet.* **13**, e1006696.
Hu, X., Zhang, W., Oliver, A. G. & Serianni, A. S. (2011). *Acta Cryst.* C**67**, o146–o150.
Klontz, E. H., Trastoy, B., Deredge, D., Fields, J. K., Li, C., Orwenyo, J., Marina, A., Beadenkopf, R., Günther, S., Flores, J., Wintrode, P. L., Wang, L.-X., Guerin, M. E. & Sundberg, E. J. (2019). *ACS Cent. Sci.* **5**, 524–538.
Kratzert, D. (2023). *FinalCif*, https://dkratzert.de/finalcif.html.
Krause, L., Herbst-Irmer, R., Sheldrick, G. M. & Stalke, D. (2015). *J. Appl. Cryst.* **48**, 3–10.
Macrae, C. F., Sovago, I., Cottrell, S. J., Galek, P. T. A., McCabe, P., Pidcock, E., Platings, M., Shields, G. P., Stevens, J. S., Towler, M. & Wood, P. A. (2020). *J. Appl. Cryst.* **53**, 226–235.
Mo, F. (1979). *Acta Chem. Scand. A*, **33**, 207–218.
Mo, F. & Jensen, L. H. (1978). *Acta Cryst.* B**34**, 1562–1569.
Moussian, B. (2019). *Adv. Exp. Med. Biol.* **1142**, 5–18.
Pandey, A., Adams, J. M., Han, S. Y. & Jafar-Nejad, H. (2022). *Cells*, **11**, 1155.
Seki, H., Huang, Y., Arakawa, T., Yamada, C., Kinoshita, T., Iwamoto, S., Higuchi, Y., Takegawa, K. & Fushinobu, S. (2019). *J. Biol. Chem.* **294**, 17143–17154.
Sheldrick, G. M. (2015*a*). *Acta Cryst.* A**71**, 3–8.
Sheldrick, G. M. (2015*b*). *Acta Cryst.* C**71**, 3–8.

supporting information

Acta Cryst. (2024). C**80**, 331-336 [https://doi.org/10.1107/S2053229624005199]

Conformational disorder in the crystal structure of methyl 2-acetamido-2-deoxy-*β*-D-glucopyranosyl-(1→4)–2-acetamido-2-deoxy-*β*-D-glucopyranoside (methyl *β*-chitobioside) methanol monosolvate

Pradip Shit, Timothy Tetrault, Wenhui Zhang, Mi-Kyung Yoon, Allen G. Oliver and Anthony S. Serianni

Computing details

Methyl 2-acetamido-2-deoxy-*β*-*D*-glucopyranosyl-(1→4)-2-acetamido-2-deoxy-*β*-*D*-glucopyranoside methanol monosolvate

Crystal data

$C_{17}H_{30}N_2O_{11}·CH_4O$
M_r = 470.47
Monoclinic, $P2_1$
a = 4.7599 (1) Å
b = 14.3223 (5) Å
c = 16.6515 (5) Å
β = 90.022 (2)°
V = 1135.18 (6) Å^3
Z = 2
$F(000)$ = 504
D_x = 1.376 Mg m^{-3}
Cu $K\alpha$ radiation, λ = 1.54178 Å
Cell parameters from 9983 reflections
θ = 2.7–71.9°
μ = 0.99 mm^{-1}
T = 260 K
Needle, colourless
0.26 × 0.04 × 0.02 mm

Data collection

Bruker Venture diffractometer
Radiation source: Incoatec Diamond micro-focus
HELIOS Multi-layer monochromator
Detector resolution: 7.41 pixels mm^{-1}
combination of ω and φ–scans
Absorption correction: numerical (SADABS2016; Krause *et al.*, 2015)
T_{min} = 0.825, T_{max} = 1.0
20006 measured reflections
4462 independent reflections
4410 reflections with $I > 2\sigma(I)$
R_{int} = 0.048
θ_{max} = 72.7°, θ_{min} = 2.7°
h = −5→5
k = −17→17
l = −20→20

Refinement

Refinement on F^2
Least-squares matrix: full
$R[F^2 > 2\sigma(F^2)]$ = 0.031
$wR(F^2)$ = 0.080
S = 1.04
4462 reflections
330 parameters
1 restraint
Primary atom site location: dual
Secondary atom site location: difference Fourier map
Hydrogen site location: mixed
H atoms treated by a mixture of independent and constrained refinement
$w = 1/[\sigma^2(F_o^2) + (0.0524P)^2 + 0.0431P]$ where $P = (F_o^2 + 2F_c^2)/3$
$(\Delta/\sigma)_{max}$ = 0.003
$\Delta\rho_{max}$ = 0.19 e Å^{-3}

$\Delta\rho_{min}$ = −0.14 e Å^{-3}

Absolute structure: Twinning involves inversion, so Flack parameter cannot be determined

Special details

Geometry. All esds (except the esd in the dihedral angle between two l.s. planes) are estimated using the full covariance matrix. The cell esds are taken into account individually in the estimation of esds in distances, angles and torsion angles; correlations between esds in cell parameters are only used when they are defined by crystal symmetry. An approximate (isotropic) treatment of cell esds is used for estimating esds involving l.s. planes.

Refinement. Refined as a 2-component inversion twin

Fractional atomic coordinates and isotropic or equivalent isotropic displacement parameters (Å^2)

	x	*y*	*z*	U_{iso}*/U_{eq}	Occ. (<1)
O1	0.6613 (6)	0.38954 (17)	1.01553 (14)	0.0445 (6)	
O3	0.6528 (6)	0.37365 (16)	0.73265 (14)	0.0412 (5)	
O5	0.7299 (6)	0.52182 (15)	0.94317 (12)	0.0396 (5)	
O6	0.9612 (16)	0.7071 (5)	0.9453 (4)	0.0641 (17)	0.5
H6O	0.875712	0.697805	0.987275	0.096*	0.5
O6A	0.538 (2)	0.6967 (5)	0.8715 (6)	0.097 (3)	0.5
H6AO	0.528968	0.753853	0.871180	0.145*	0.5
O8	0.3233 (5)	0.2240 (2)	0.9067 (2)	0.0590 (8)	
N1	0.7583 (5)	0.27620 (17)	0.87908 (16)	0.0299 (5)	
H1N	0.932 (8)	0.266 (2)	0.8755 (19)	0.017 (7)*	
C1	0.7936 (7)	0.4255 (2)	0.94888 (17)	0.0330 (6)	
H1A	0.997167	0.416705	0.953441	0.040*	
C2	0.6822 (6)	0.37358 (19)	0.87507 (18)	0.0293 (5)	
H2A	0.476738	0.378155	0.874899	0.035*	
C3	0.7936 (6)	0.4179 (2)	0.79753 (17)	0.0298 (6)	
H3A	0.995667	0.405910	0.793219	0.036*	
C4	0.7431 (7)	0.52381 (19)	0.79937 (17)	0.0296 (5)	
H4A	0.540824	0.536263	0.796932	0.036*	
C5	0.8640 (8)	0.5658 (2)	0.87643 (17)	0.0379 (6)	
H5A	1.066193	0.553185	0.878652	0.046*	
C6	0.8160 (12)	0.6693 (3)	0.8831 (2)	0.0593 (11)	
H6A	0.873382	0.699202	0.833542	0.071*	0.5
H6B	0.617058	0.681054	0.890635	0.071*	0.5
H6C	0.876044	0.689708	0.935970	0.071*	0.5
H6D	0.932925	0.700711	0.843857	0.071*	0.5
C7	0.8083 (12)	0.4062 (3)	1.0894 (2)	0.0541 (10)	
H7A	0.723974	0.370095	1.131539	0.081*	
H7B	0.797678	0.471347	1.102649	0.081*	
H7C	1.001519	0.388351	1.083378	0.081*	
C8	0.5760 (6)	0.2082 (2)	0.8968 (2)	0.0372 (7)	
C9	0.6950 (8)	0.1115 (3)	0.9016 (3)	0.0536 (9)	
H9A	0.609485	0.078600	0.945515	0.080*	
H9B	0.894259	0.114941	0.910051	0.080*	
H9C	0.657534	0.078887	0.852381	0.080*	
O1′	0.8809 (4)	0.57052 (15)	0.73397 (12)	0.0298 (4)	

O3′	0.7196 (5)	0.74058 (15)	0.48957 (14)	0.0367 (5)
H3′O	0.567 (12)	0.759 (4)	0.471 (3)	0.052 (13)*
H3O	0.715 (10)	0.398 (3)	0.685 (3)	0.046 (11)*
O4′	0.4803 (6)	0.56213 (19)	0.42887 (16)	0.0499 (6)
H4′O	0.551 (11)	0.605 (4)	0.393 (3)	0.052 (12)*
O5′	0.8318 (5)	0.49753 (14)	0.61404 (12)	0.0297 (4)
O6′	0.7734 (5)	0.32150 (16)	0.54828 (16)	0.0395 (5)
H6′O	0.909 (16)	0.295 (5)	0.540 (4)	0.08 (2)*
O7′	1.1510 (5)	0.7998 (2)	0.6826 (2)	0.0559 (7)
N1′	0.7139 (5)	0.74593 (17)	0.66216 (15)	0.0287 (5)
H1N′	0.522 (8)	0.758 (2)	0.6661 (18)	0.020 (7)*
C1′	0.7340 (6)	0.5731 (2)	0.66160 (16)	0.0280 (5)
H1′A	0.531861	0.566904	0.671392	0.034*
C2′	0.7956 (5)	0.66437 (18)	0.61688 (16)	0.0267 (5)
H2′A	0.997740	0.667805	0.606156	0.032*
C3′	0.6387 (6)	0.6623 (2)	0.53637 (17)	0.0293 (6)
H3′A	0.436964	0.667216	0.547368	0.035*
C4′	0.6892 (6)	0.5726 (2)	0.48892 (16)	0.0317 (6)
H4′A	0.874727	0.575294	0.463538	0.038*
C5′	0.6709 (6)	0.48547 (19)	0.54181 (17)	0.0299 (6)
H5′A	0.474313	0.472657	0.555322	0.036*
C6′	0.7956 (8)	0.4029 (2)	0.49838 (19)	0.0373 (7)
H6′A	0.696242	0.392679	0.448283	0.045*
H6′B	0.991389	0.415061	0.486059	0.045*
C7′	0.8984 (6)	0.8097 (2)	0.6888 (2)	0.0330 (6)
C8′	0.7740 (8)	0.8961 (2)	0.7253 (2)	0.0461 (8)
H8′A	0.846644	0.950160	0.698249	0.069*
H8′B	0.822429	0.898956	0.781168	0.069*
H8′C	0.573311	0.894426	0.719681	0.069*
O1S	0.5403 (7)	0.6821 (2)	0.3019 (2)	0.0632 (8)
H1S	0.474933	0.734452	0.294896	0.095*
C1S	0.8289 (14)	0.6839 (6)	0.2880 (3)	0.091 (2)
H1SA	0.900524	0.621240	0.287904	0.136*
H1SB	0.919732	0.719208	0.329534	0.136*
H1SC	0.865150	0.712465	0.236866	0.136*

Atomic displacement parameters (Å²)

	U^{11}	U^{22}	U^{33}	U^{12}	U^{13}	U^{23}
O1	0.0584 (14)	0.0455 (13)	0.0297 (11)	−0.0091 (12)	0.0059 (10)	0.0026 (10)
O3	0.0594 (15)	0.0319 (10)	0.0324 (11)	−0.0080 (10)	−0.0036 (11)	−0.0007 (9)
O5	0.0583 (14)	0.0326 (11)	0.0280 (9)	0.0049 (10)	0.0080 (10)	−0.0016 (8)
O6	0.094 (4)	0.052 (3)	0.046 (3)	−0.032 (3)	0.010 (3)	−0.018 (3)
O6A	0.141 (7)	0.046 (3)	0.103 (6)	0.048 (4)	0.061 (6)	0.013 (4)
O8	0.0259 (12)	0.0619 (17)	0.089 (2)	−0.0020 (12)	0.0048 (13)	0.0188 (15)
N1	0.0206 (11)	0.0304 (12)	0.0387 (12)	0.0011 (9)	0.0013 (10)	0.0028 (10)
C1	0.0382 (15)	0.0302 (14)	0.0307 (13)	0.0011 (12)	0.0014 (13)	0.0019 (11)
C2	0.0243 (11)	0.0288 (13)	0.0348 (14)	0.0002 (10)	0.0010 (12)	0.0034 (11)

C3	0.0308 (14)	0.0298 (13)	0.0287 (12)	0.0002 (11)	0.0019 (11)	−0.0009 (10)
C4	0.0324 (13)	0.0272 (12)	0.0292 (12)	0.0011 (11)	0.0042 (12)	0.0014 (11)
C5	0.0537 (17)	0.0316 (14)	0.0285 (13)	−0.0022 (14)	0.0044 (14)	−0.0013 (12)
C6	0.114 (4)	0.0319 (16)	0.0321 (16)	−0.002 (2)	0.003 (2)	−0.0041 (14)
C7	0.088 (3)	0.0457 (17)	0.0290 (14)	0.0033 (19)	−0.0018 (18)	0.0021 (13)
C8	0.0280 (15)	0.0366 (15)	0.0472 (17)	−0.0027 (12)	0.0007 (13)	0.0083 (13)
C9	0.0460 (19)	0.0336 (16)	0.081 (3)	−0.0041 (15)	0.0046 (19)	0.0092 (17)
O1′	0.0318 (9)	0.0296 (9)	0.0280 (9)	−0.0027 (9)	−0.0009 (8)	0.0015 (8)
O3′	0.0347 (12)	0.0325 (10)	0.0429 (11)	−0.0005 (9)	−0.0012 (9)	0.0122 (9)
O4′	0.0624 (16)	0.0430 (13)	0.0442 (12)	−0.0106 (13)	−0.0234 (12)	0.0060 (11)
O5′	0.0345 (9)	0.0254 (8)	0.0291 (9)	0.0054 (7)	−0.0038 (9)	−0.0015 (7)
O6′	0.0369 (11)	0.0269 (10)	0.0547 (14)	0.0000 (9)	−0.0015 (10)	−0.0045 (10)
O7′	0.0233 (11)	0.0536 (15)	0.091 (2)	−0.0022 (11)	0.0001 (12)	−0.0168 (14)
N1′	0.0191 (11)	0.0274 (11)	0.0396 (12)	0.0016 (9)	0.0012 (9)	−0.0023 (9)
C1′	0.0288 (12)	0.0257 (11)	0.0294 (12)	0.0003 (12)	0.0010 (10)	−0.0003 (11)
C2′	0.0239 (11)	0.0238 (11)	0.0323 (12)	−0.0001 (10)	0.0029 (11)	0.0029 (11)
C3′	0.0229 (12)	0.0262 (12)	0.0389 (14)	0.0009 (11)	−0.0014 (11)	0.0072 (12)
C4′	0.0345 (13)	0.0332 (13)	0.0274 (12)	−0.0025 (13)	−0.0044 (11)	0.0022 (12)
C5′	0.0308 (14)	0.0275 (13)	0.0314 (13)	−0.0032 (11)	−0.0061 (12)	−0.0009 (10)
C6′	0.0444 (17)	0.0323 (14)	0.0353 (14)	0.0014 (13)	−0.0044 (14)	−0.0053 (12)
C7′	0.0313 (15)	0.0301 (14)	0.0376 (16)	−0.0011 (12)	−0.0037 (12)	0.0011 (12)
C8′	0.0425 (17)	0.0369 (15)	0.0587 (19)	0.0027 (14)	−0.0063 (16)	−0.0160 (16)
O1S	0.0670 (18)	0.0633 (19)	0.0594 (16)	0.0089 (16)	−0.0009 (15)	0.0201 (15)
C1S	0.070 (3)	0.141 (6)	0.061 (3)	−0.016 (4)	0.007 (3)	0.022 (3)

Geometric parameters (Å, º)

O1—C1	1.376 (4)	C9—H9C	0.9600
O1—C7	1.435 (5)	O1′—C1′	1.394 (3)
O3—C3	1.420 (4)	O3′—C3′	1.419 (3)
O3—H3O	0.91 (5)	O3′—H3′O	0.83 (6)
O5—C1	1.416 (3)	O4′—C4′	1.418 (4)
O5—C5	1.428 (4)	O4′—H4′O	0.92 (5)
O6—C6	1.356 (8)	O5′—C1′	1.420 (3)
O6—H6O	0.8200	O5′—C5′	1.436 (4)
O6A—C6	1.393 (12)	O6′—C6′	1.436 (4)
O6A—H6AO	0.8200	O6′—H6′O	0.76 (8)
O8—C8	1.235 (4)	O7′—C7′	1.215 (4)
N1—C8	1.338 (4)	N1′—C7′	1.342 (4)
N1—C2	1.443 (4)	N1′—C2′	1.444 (4)
N1—H1N	0.84 (4)	N1′—H1N′	0.93 (4)
C1—C2	1.531 (4)	C1′—C2′	1.533 (4)
C1—H1A	0.9800	C1′—H1′A	0.9800
C2—C3	1.534 (4)	C2′—C3′	1.535 (4)
C2—H2A	0.9800	C2′—H2′A	0.9800
C3—C4	1.536 (3)	C3′—C4′	1.527 (4)
C3—H3A	0.9800	C3′—H3′A	0.9800
C4—O1′	1.437 (4)	C4′—C5′	1.530 (4)

C4—C5	1.529 (4)	C4′—H4′A	0.9800
C4—H4A	0.9800	C5′—C6′	1.508 (4)
C5—C6	1.503 (5)	C5′—H5′A	0.9800
C5—H5A	0.9800	C6′—H6′A	0.9700
C6—H6A	0.9700	C6′—H6′B	0.9700
C6—H6B	0.9700	C7′—C8′	1.501 (4)
C6—H6C	0.9700	C8′—H8′A	0.9600
C6—H6D	0.9700	C8′—H8′B	0.9600
C7—H7A	0.9600	C8′—H8′C	0.9600
C7—H7B	0.9600	O1S—C1S	1.393 (7)
C7—H7C	0.9600	O1S—H1S	0.8200
C8—C9	1.499 (5)	C1S—H1SA	0.9600
C9—H9A	0.9600	C1S—H1SB	0.9600
C9—H9B	0.9600	C1S—H1SC	0.9600

C1—O1—C7	113.9 (3)	H9A—C9—H9C	109.5
C3—O3—H3O	109 (3)	H9B—C9—H9C	109.5
C1—O5—C5	112.7 (2)	C1′—O1′—C4	116.0 (2)
C6—O6—H6O	109.5	C3′—O3′—H3′O	103 (3)
C6—O6A—H6AO	109.5	C4′—O4′—H4′O	98 (3)
C8—N1—C2	123.5 (2)	C1′—O5′—C5′	112.6 (2)
C8—N1—H1N	121 (2)	C6′—O6′—H6′O	103 (5)
C2—N1—H1N	115 (2)	C7′—N1′—C2′	123.1 (2)
O1—C1—O5	108.7 (3)	C7′—N1′—H1N′	119 (2)
O1—C1—C2	107.9 (2)	C2′—N1′—H1N′	117 (2)
O5—C1—C2	110.2 (2)	O1′—C1′—O5′	107.3 (2)
O1—C1—H1A	110.0	O1′—C1′—C2′	110.3 (2)
O5—C1—H1A	110.0	O5′—C1′—C2′	108.4 (2)
C2—C1—H1A	110.0	O1′—C1′—H1′A	110.2
N1—C2—C1	110.2 (2)	O5′—C1′—H1′A	110.2
N1—C2—C3	110.6 (2)	C2′—C1′—H1′A	110.2
C1—C2—C3	110.8 (2)	N1′—C2′—C1′	112.6 (2)
N1—C2—H2A	108.4	N1′—C2′—C3′	109.9 (2)
C1—C2—H2A	108.4	C1′—C2′—C3′	108.3 (2)
C3—C2—H2A	108.4	N1′—C2′—H2′A	108.6
O3—C3—C2	107.0 (2)	C1′—C2′—H2′A	108.6
O3—C3—C4	112.5 (2)	C3′—C2′—H2′A	108.6
C2—C3—C4	109.8 (2)	O3′—C3′—C4′	109.7 (2)
O3—C3—H3A	109.2	O3′—C3′—C2′	109.4 (2)
C2—C3—H3A	109.2	C4′—C3′—C2′	113.1 (2)
C4—C3—H3A	109.2	O3′—C3′—H3′A	108.2
O1′—C4—C5	106.3 (2)	C4′—C3′—H3′A	108.2
O1′—C4—C3	111.9 (2)	C2′—C3′—H3′A	108.2
C5—C4—C3	110.3 (2)	O4′—C4′—C3′	110.1 (3)
O1′—C4—H4A	109.4	O4′—C4′—C5′	106.3 (2)
C5—C4—H4A	109.4	C3′—C4′—C5′	112.3 (2)
C3—C4—H4A	109.4	O4′—C4′—H4′A	109.4
O5—C5—C6	108.0 (3)	C3′—C4′—H4′A	109.4

O5—C5—C4	108.1 (3)	C5′—C4′—H4′A	109.4
C6—C5—C4	113.1 (3)	O5′—C5′—C6′	106.6 (2)
O5—C5—H5A	109.2	O5′—C5′—C4′	110.7 (2)
C6—C5—H5A	109.2	C6′—C5′—C4′	109.9 (3)
C4—C5—H5A	109.2	O5′—C5′—H5′A	109.8
O6—C6—C5	111.9 (5)	C6′—C5′—H5′A	109.8
O6A—C6—C5	114.3 (5)	C4′—C5′—H5′A	109.8
O6—C6—H6A	109.2	O6′—C6′—C5′	109.3 (3)
C5—C6—H6A	109.2	O6′—C6′—H6′A	109.8
O6—C6—H6B	109.2	C5′—C6′—H6′A	109.8
C5—C6—H6B	109.2	O6′—C6′—H6′B	109.8
H6A—C6—H6B	107.9	C5′—C6′—H6′B	109.8
O6A—C6—H6C	108.7	H6′A—C6′—H6′B	108.3
C5—C6—H6C	108.7	O7′—C7′—N1′	122.7 (3)
O6A—C6—H6D	108.7	O7′—C7′—C8′	121.4 (3)
C5—C6—H6D	108.7	N1′—C7′—C8′	115.9 (3)
H6C—C6—H6D	107.6	C7′—C8′—H8′A	109.5
O1—C7—H7A	109.5	C7′—C8′—H8′B	109.5
O1—C7—H7B	109.5	H8′A—C8′—H8′B	109.5
H7A—C7—H7B	109.5	C7′—C8′—H8′C	109.5
O1—C7—H7C	109.5	H8′A—C8′—H8′C	109.5
H7A—C7—H7C	109.5	H8′B—C8′—H8′C	109.5
H7B—C7—H7C	109.5	C1S—O1S—H1S	109.5
O8—C8—N1	121.8 (3)	O1S—C1S—H1SA	109.5
O8—C8—C9	122.0 (3)	O1S—C1S—H1SB	109.5
N1—C8—C9	116.1 (3)	H1SA—C1S—H1SB	109.5
C8—C9—H9A	109.5	O1S—C1S—H1SC	109.5
C8—C9—H9B	109.5	H1SA—C1S—H1SC	109.5
H9A—C9—H9B	109.5	H1SB—C1S—H1SC	109.5
C8—C9—H9C	109.5		

C7—O1—C1—O5	−81.3 (3)	C5—C4—O1′—C1′	−154.8 (2)
C7—O1—C1—C2	159.2 (3)	C3—C4—O1′—C1′	84.7 (3)
C5—O5—C1—O1	178.7 (3)	C4—O1′—C1′—O5′	−95.8 (3)
C5—O5—C1—C2	−63.3 (3)	C4—O1′—C1′—C2′	146.2 (2)
C8—N1—C2—C1	105.6 (3)	C5′—O5′—C1′—O1′	172.6 (2)
C8—N1—C2—C3	−131.5 (3)	C5′—O5′—C1′—C2′	−68.3 (3)
O1—C1—C2—N1	−64.1 (3)	C7′—N1′—C2′—C1′	115.7 (3)
O5—C1—C2—N1	177.4 (2)	C7′—N1′—C2′—C3′	−123.4 (3)
O1—C1—C2—C3	173.1 (2)	O1′—C1′—C2′—N1′	−60.3 (3)
O5—C1—C2—C3	54.6 (3)	O5′—C1′—C2′—N1′	−177.6 (2)
N1—C2—C3—O3	64.8 (3)	O1′—C1′—C2′—C3′	177.8 (2)
C1—C2—C3—O3	−172.7 (2)	O5′—C1′—C2′—C3′	60.6 (3)
N1—C2—C3—C4	−172.9 (2)	N1′—C2′—C3′—O3′	63.7 (3)
C1—C2—C3—C4	−50.4 (3)	C1′—C2′—C3′—O3′	−172.8 (2)
O3—C3—C4—O1′	−69.8 (3)	N1′—C2′—C3′—C4′	−173.7 (2)
C2—C3—C4—O1′	171.2 (2)	C1′—C2′—C3′—C4′	−50.2 (3)
O3—C3—C4—C5	172.1 (2)	O3′—C3′—C4′—O4′	−75.0 (3)

C2—C3—C4—C5	53.1 (3)	C2′—C3′—C4′—O4′	162.6 (2)
C1—O5—C5—C6	−172.0 (3)	O3′—C3′—C4′—C5′	166.9 (2)
C1—O5—C5—C4	65.3 (3)	C2′—C3′—C4′—C5′	44.4 (3)
O1′—C4—C5—O5	179.4 (2)	C1′—O5′—C5′—C6′	−179.4 (2)
C3—C4—C5—O5	−59.1 (3)	C1′—O5′—C5′—C4′	61.1 (3)
O1′—C4—C5—C6	59.8 (4)	O4′—C4′—C5′—O5′	−167.9 (2)
C3—C4—C5—C6	−178.7 (3)	C3′—C4′—C5′—O5′	−47.5 (3)
O5—C5—C6—O6	69.8 (5)	O4′—C4′—C5′—C6′	74.5 (3)
C4—C5—C6—O6	−170.6 (4)	C3′—C4′—C5′—C6′	−165.1 (3)
O5—C5—C6—O6A	−68.4 (5)	O5′—C5′—C6′—O6′	60.7 (3)
C4—C5—C6—O6A	51.3 (6)	C4′—C5′—C6′—O6′	−179.2 (3)
C2—N1—C8—O8	4.1 (5)	C2′—N1′—C7′—O7′	−6.3 (5)
C2—N1—C8—C9	−177.5 (3)	C2′—N1′—C7′—C8′	172.3 (3)

Hydrogen-bond geometry (Å, º)

D—H···*A*	*D*—H	H···*A*	*D*···*A*	*D*—H···*A*
O6^{a}—H6*O*a···O8^{i}	0.82	2.04	2.823 (7)	160
N1—H1*N*···O8^{ii}	0.84 (4)	2.02 (4)	2.829 (4)	160 (3)
C9—H9*A*···O5^{iii}	0.96	2.59	3.525 (5)	165
C9—H9*B*···O8^{ii}	0.96	2.57	3.398 (5)	144
O3′—H3′*O*···O6′^{iv}	0.83 (6)	1.88 (6)	2.692 (3)	165 (5)
O3—H3*O*···O5′	0.91 (5)	1.94 (5)	2.789 (3)	155 (4)
O3—H3*O*···O6′	0.91 (5)	2.55 (5)	3.212 (4)	130 (4)
O4′—H4′*O*···O1*S*	0.92 (5)	1.88 (5)	2.739 (4)	155 (5)
O6′—H6′*O*···O3′^{v}	0.76 (8)	1.99 (8)	2.750 (4)	173 (7)
N1′—H1*N*′···O7′^{vi}	0.93 (4)	1.88 (4)	2.808 (3)	171 (3)
C6′—H6′*A*···O7′^{v}	0.97	2.66	3.366 (5)	130
C8′—H8′*C*···O7′^{vi}	0.96	2.50	3.347 (5)	147
O1*S*—H1*S*···O3^{iv}	0.82	2.13	2.950 (4)	173
C1*S*—H1*SC*···O8^{iv}	0.96	2.56	3.371 (7)	142

Symmetry codes: (i) −*x*+1, *y*+1/2, −*z*+2; (ii) *x*+1, *y*, *z*; (iii) −*x*+1, *y*−1/2, −*z*+2; (iv) −*x*+1, *y*+1/2, −*z*+1; (v) −*x*+2, *y*−1/2, −*z*+1; (vi) *x*−1, *y*, *z*.